Colloids and Surfaces B: Biointerfaces 73 (2009) 42–50

Contents lists available at ScienceDirect

Colloids and Surfaces B: Biointerfaces

journal homepage: www.elsevier.com/locate/colsurfb

Study of the effect of Na^+ and Ca^{2+} ion concentration on the structure of an asymmetric DPPC/DPPC + DPPS lipid bilayer by molecular dynamics simulation

Rodolfo D. Porasso[a,b], J.J. López Cascales[a,*]

[a] Universidad Politécnica de Cartagena, Grupo de Bioinformática y Macromoléculas (BioMac) Aulario II, Campus de Alfonso XIII, 30203 Cartagena, Murcia, Spain
[b] Instituto de Matemática Aplicada San Luis (IMASL), Departamento de Física, Universidad Nacional de San Luis/CONICET, D5700HHW San Luis, Argentina

ARTICLE INFO

Article history:
Received 30 January 2009
Received in revised form 24 April 2009
Accepted 28 April 2009
Available online 9 May 2009

Keywords:
Asymmetric membrane
DPPC
DPPS
Ionic strength
MD simulation

ABSTRACT

A molecular dynamics simulation study of the steady and dynamic properties of an asymmetric phospholipid bilayer was carried out in the presence of sodium or calcium ions. The asymmetric lipid bilayer was seen to resemble a cellular membrane of an eukaryotic cell, which was modeled by dipalmitoylphosphatidylcholine (DPPC) and dipalmitoylphosphatidylserine (DPPS), placing the DPPS in one of the two leaflets of the lipid bilayer.

From a numerical analysis of the simulated trajectories, information was obtained with atomic resolution for both membrane leaflet concerning the effect of bilayer asymmetry on different properties of the lipid/water interface, such as the translational diffusion coefficient and rotational relaxation time of the water molecules, lipid hydration, and residence time of water around different lipid atoms. In addition, information related to lipid conformation, and lipid–lipid interactions was also analyzed.

1. Introduction

Phospholipids play an undoubted role in the function of biological cells in which they control the diffusion of small molecules between the interior and the exterior of the membrane, and provide a suitable environment for other molecules embedded or anchored in the membrane [1], such as proteins, polysaccharides or cholesterol. As regards the membrane structure of eukaryotic cells, lipids are asymmetrically distributed between the inner and the outer leaflets of the membrane. Thus, phosphatidylserine (PS) lipids are asymmetrically located in the inner leaflet of the membrane, where the loss of asymmetry seems to be a hallmark of the early stages of cell apoptosis [2], whereby apoptotic cells are removed from the blood stream. Thus, proteins have been reported to bind to exposed PS molecules on dying cells, some of these molecules bind to PS directly and some via bridging molecules [3,4].

It is also well known that, under physiological conditions, lipids in biological membranes interact with aqueous solution containing different types of ions, for example Na^+, K^+, Ca^{2+}or Mg^{2+}, monovalent cations (Na^+ and K^+) modulate the properties of the plasma membrane, whereas divalent ions such us calcium (Ca^{2+}) play an important role in the mitochondrial membranes [5,6].

Providing insight into this subject with atomic detail, the molecular dynamic (MD) simulations technique has emerged during recent decades as a powerful tool for investigating, the behavior of phospholipid bilayers [7,8] at molecular level. Many MD simulations have recently been reported related to the structure and dynamics of symmetric phospholipid bilayers, where only one type of phospholipids was distributed on both leaflets of the membrane [9–17]. In this regard, several MD simulations of symmetric bilayers in the presence of monovalent ions have been reported: Pandit et al. [15] studied the effect of NaCl on a dipalmitoylphosphatidylcholine (DPPC), Sachs et al. [18] studied the effect of monovalent Na^+ salts on a palmitoyl-oleoyl-phosphatidylcholine (POPC), Mukhopadhyay et al. [17] investigated the effect of Na^+ counterions and NaCl on a palmitoyl-oleoyl phosphatidylserine (POPS) bilayer, Shinoda et al. [19] presented the interaction between an archeal lipid diphytanylphosphatidylcholine (DPhPC) with sodium chloride, and Gurtovenko and Vattulainen [20] shown the effect of NaCl and KCl on POPC and palmitoyl-oleoyl-phosphatidylethanolamine (POPE) bilayers. Many studies have been conducted during the last decades regarding the interaction between phospholipid bilayers and divalent ions. Thus, the effect of Ca^{2+} on different phosphatidylcholine (PC) bilayers has been studied using different techniques: MD simulation [21,22], diffraction method [23–28], calorimetry [29,30], H NMR [31,5,32,33], interbilayer force measuring [34], infrared spectroscopy [6] and particle electrophoresis [35,36].

Nevertheless, the study of asymmetric bilayers remains a topic of special relevance due to its interest for the field of biological membranes. In this setting, a model of an asymmetric lipid bilayer was recently proposed by López Cascales et al. [37], in which DPPS was asymmetrically distributed on only one of the two leaflets of

* Corresponding author. Tel.: +34 968325567; fax: +34 968325931.
E-mail address: javier.lopez@upct.es (J.J. López Cascales).

0927-7765/$ – see front matter © 2009 Elsevier B.V. All rights reserved.
doi:10.1016/j.colsurfb.2009.04.028

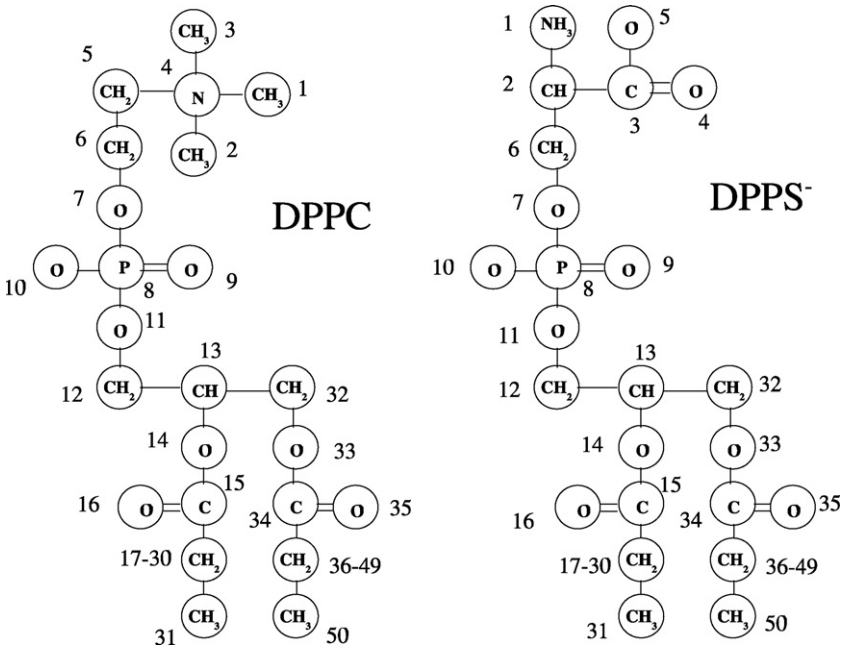

Fig. 1. Atomic numeration of DPPC and DPPS. This atomic numeration is used throughout the paper.

a DPPC bilayer. This model was taken as the starting point for the studies described in this work.

In the present study, we focus our interest on the effect of the monovalent and divalent cations, $Na^+$and Ca^{2+}, on the structure of the lipid/water interface and the rearrangements that take place in the phospholipid bilayer as a consequence of the presence of these ions in solution. Thus, different lipid hydration rates on both sides of the lipid bilayer, lipid–lipid charge bridge formation, lipid head group orientation, the translational diffusion coefficient and rotational relaxation time of water on both sides of the membrane and the translational diffusion coefficient of ions from bulk to the lipid/water interface were investigated.

Finally with the aim of investigating the real effect of monovalent and divalent cations on a phospholipid bilayer, the ion concentrations have been expressed in normal concentrations (N) instead of molar ones (M), in order to keep the charge density in solution constant.[1]

2. Methods and models

2.1. Setting up the system

Four molecular dynamics simulations were carried out with atomic detail of a model of asymmetric membrane composed of DPPC/DPPS in aqueous solution with either monovalent or divalent ions at different concentrations. In addition, a DPPC bilayer in water was taken as reference to validate the force field used in our simulations. Thus, the following five simulations were carried out:

1. 288DPPC/9956 water molecules.
2. 216DPPC/48DPPS/48Na^+/9908 water molecules, in the absence of salt. Sodium ions were used to keep the charge balance of the system.
3. 216DPPC/48DPPS/96Na^+/48Cl^-/9812 water molecules, corresponding to 0.25N in NaCl.
4. 216DPPC/48DPPS/24Ca^{2+}, 9932 water molecules, in the absence of salt. Calcium ions were used to keep the charge balance of the system.
5. 216DPPC/48DPPS/48Ca^{2+}/48Cl^-/9860 water molecules, corresponding to 0.25N in $CaCl_2$.

To construct the system, we started from a DPPC molecule (Fig. 1), in which the long molecular axis was oriented perpendicularly to the membrane face (x, $y$plane). Next, this molecule was randomly rotated and copied 144 times on both sides of the lipid bilayer and water was added to fill in the gaps above and below the phospholipid leaflet, to hydrate the lipid head groups.

The asymmetry of lipid distribution was generated by substitution of 48 DPPCs in one of the two leaflets by 48 DPPSs (Fig. 1). In addition, 24 DPPCs of the opposite leaflet were removed in order to reproduce the area per lipid of a pure DPPC bilayer thus avoiding any excess in the surface pressure, such as it was described in detail elsewhere [37]. To balance the net charge associated with the presence of DPPS, 48 or 24 water molecules were randomly substituted by Na^+or Ca^{2+}, respectively. This number of sodium and calcium ions must remain constant independently of the salt concentration to maintain the electro-neutrality of the system, i.e. in presence of any salt concentration in solution, the total cation number will not be exactly balanced with anions in solution. To consider 0.25N in NaCl or $CaCl_2$, additional 96 or 72 water molecules were substituted (48 Na^++ 48 Cl^- and 24 Ca^{2+} + 48 Cl^-, respectively). Once the five starting systems have been generated, a minimization process was applied to each system to remove the excess of energy associated to overlaps between neighboring atoms of the system.

The GROMACS 3.3.2 package [38,39] was used to carry out the molecular dynamics simulations. The force field parameters and electrostatic charge distribution of the DPPC and DPPS have already been reported elsewhere [12,14]. In all the simulations the time step was 2 fs, while a cutoff of 1.0 nm was used for calculating the Lennard–Jones interactions. The electrostatic interaction were evaluated using the Ewald particle mesh method [40,41]. The real space interaction was evaluated using a 0.9 nm cutoff, and the reciprocal space interaction using a 0.12 nm grid with a fourth-order spline interpolation. Simulations were performed using an anisotropic

[1] Notice that normality = molarity × charge.

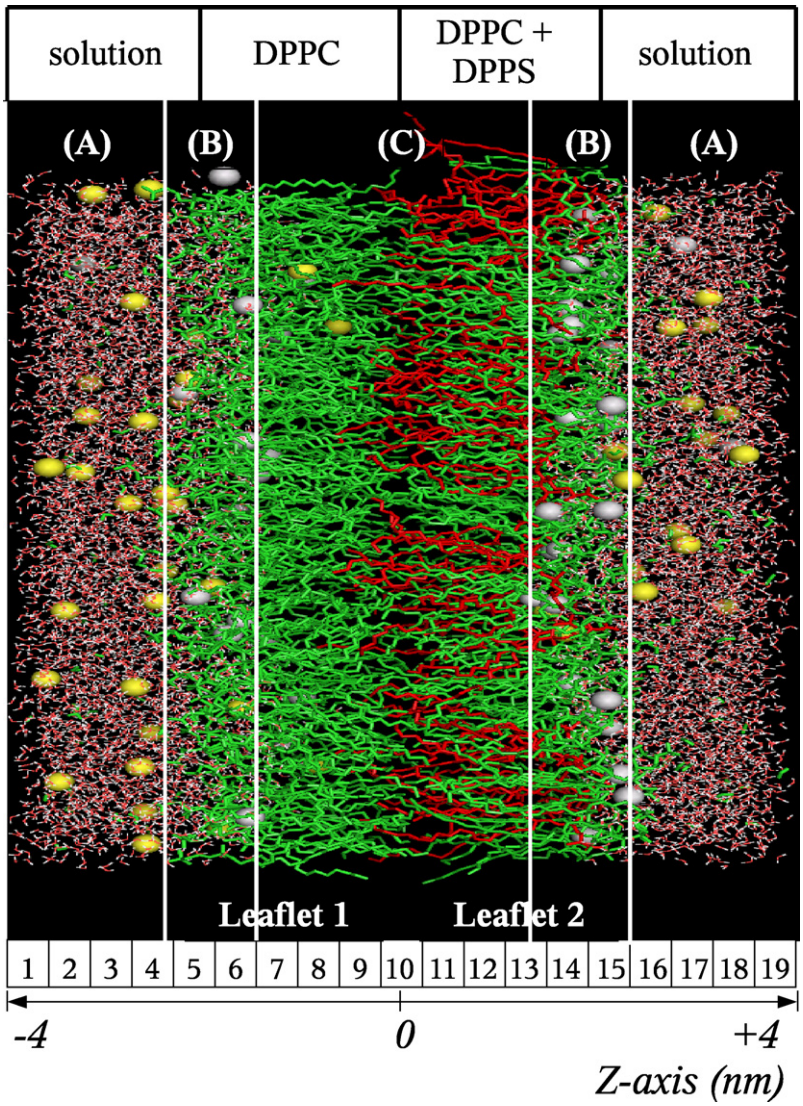

Fig. 2. Snapshot of the membrane corresponding to 0.25 N $CaCl_2$. This snapshot was divided into 19 slabs parallel to the membrane, and the origin of the *z*-axis was placed in the middle of the lipid bilayer. White beads correspond to calcium ions (Ca^{2+}), yellow beads correspond to chloride ions (Cl^-) and red and white sticks correspond to water molecules. $DPPS^-$ are colored red, while DPPC are in green wireframes. Leaflet 1 refers to the leaflet composed only of DPPC and leaflet 2 is composed of DPPC + DPPS, such as we will refer to through the text. The system was also divided in three generic zones: (A) bulk solution, (B) lipid heads and (C) lipid hydrocarbon tails. (For interpretation of the references to color in this figure legend, the reader is referred to the web version of the article.)

coupling pressure, in a pressure bath of 1 atm, which allowed the independent fluctuation of each axis of the computer box. Each component of the system (i.e. lipids, ions and water) was coupled to an external temperature coupling bath at 350 K, which is well above the transition temperatures of 314 and 326 K for DPPC [42,43] and DPPS [44,45] bilayers, respectively. All the MD simulations were carried out using periodic boundary conditions. The SPCE [46] water model was used in the simulations. Thus, trajectories of 20 ns length were simulated for all the cases described above.

Fig. 2 shows a snapshot of the membrane corresponding to 0.25N in $CaCl_2$, which was generated following the procedure described above. In these conditions, the systems achieved an equilibrated state after 5 ns of simulation considering the surface area per lipid for the DPPC leaflet in absence of DPPS, in 0.25N $CaCl_2$. This result contrasts with the results presented by Bockmann and Grubmuller [16], who asserted that a minimum trajectory length of 100 ns is required to equilibrate the system. Thus, data from the last 15 ns of simulation were used for analysis.

The dimensions of the periodical computing boxes (*X*, *Y* and *Z*, in nm) corresponding to the five cases studied above were the following: (1) $(8.79 \pm 0.06, 11.52 \pm 0.04, 6.96 \pm 0.12)$, (2) $(8.87 \pm 0.04, 9.20 \pm 0.05, 7.57 \pm 0.15)$, (3) $(8.31 \pm 0.07, 9.24 \pm 0.07, 7.67 \pm 0.21)$, (4) $(8.97 \pm 0.07, 9.05 \pm 0.07, 7.84 \pm 0.13)$ and (5) $(6.89 \pm 0.05, 11.58 \pm 0.09, 8.00 \pm 0.12)$.

All these simulations were carried out using processors of a parallel HP ES 45 cluster Alpha Server.

3. Results and discussion

3.1. Density and surface area per lipid

Fig. 3 displays the atomic density across the phospholipid bilayers. These figures show how the asymmetry of the system introduces the expected asymmetry in the atomic distribution on both sides of the membrane.

The values measured for the surface area of the leaflet formed by pure DPPC is summarized in Table 1. From these values, we observe how the surface area agrees with experimental data of DPPC bilayers in pure water [47] at 350 K. It is also observed how salt shrinks the surface area of DPPC, in good agreement with previous results

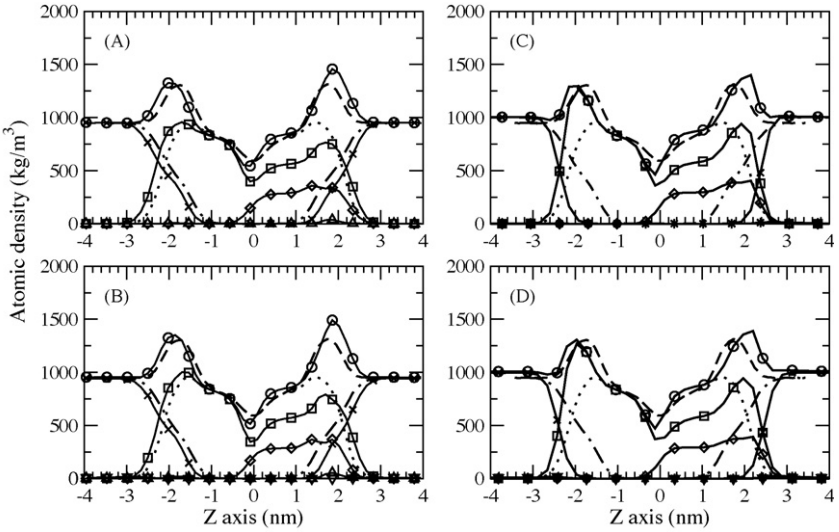

Fig. 3. Density profile across the lipid bilayer: (A) bilayer in pure water with sodium ions as counterions, (B) bilayer in 0.25N NaCl, (C) bilayer in pure water with calcium ions as counterions and (D) bilayer in 0.25N $CaCl_2$. (◯) total density, (□) DPPC density, (◊) DPPS density, (△) NA^+density, (∗) Ca^{2+} density, (▽) Cl^- density, (×) H_2O. The density profile of a pure DPPC bilayer in water in absence of ions was included as control: (– –) Total density, (···) DPPC density, (–·–) H_2O density. *Z*-axis corresponds to Fig. 2.

of DPPC bilayers in presence of salt [15,18]. Our results show how the level of shrinking of the surface area of lipids is almost the same in the presence of NaCl and $CaCl_2$at normal concentrations (N).

3.2. Lipid–lipid interactions

The radial distribution function $g(r)$ is often used to identify interaction between neighboring atoms. In this regard, the radial distribution function $g(r)$ is defined as

$$g(r) = \frac{N(r)}{4\pi r^2 \rho \delta r} \quad (1)$$

where, $N(r)$ is the number of atoms in a spherical shell at distance r and thickness δr from a reference atom, and ρ is the number density taken as the ratio of atoms to the volume of the computing box.

To confirm the possible existence of charge bridges between neighboring phospholipids, the radial distribution function $g(r)$ between atoms of different lipids was investigated. Thus, the amino group NH_3 of the DPPS (atom 1, Fig. 1) was assigned as the reference atom to calculate the radial distribution function, and several oxygen atoms of the DPPC (as potential charge bridge donors) were investigated. Fig. 4 depicts the radial distribution function of the phosphate oxygen (atom 10, Fig. 1), and the carbonyl oxygen group (atom 16, Fig. 1) around the amino group $NH_3$of DPPS (see Fig. 1). From the results obtained in Fig. 4, we conclude that the charge bridges between neighboring lipids are strongly affected by the salt in solution: higher salt concentrations promote bridge formation between the DPPC oxygen carbonyl and the DPPS amino groups, while in the absence of salt, the charge bridges with phosphate oxygens prevail over the carbonyl groups. This effect is strongly related with the fact that higher salt concentrations promote cation penetration into the membrane and hence, the formation of bridges with carbonyl groups, which agrees closely with the results obtained by Pandit et al. [15].

Table 1
Summary of the molecular dynamics simulation of the lipid bilayer at different ionic strengths.

System	$\langle A \rangle$ (nm^2) [a]	$\langle \theta \rangle$ (°) [b]		Hydration number [c]	
		Leaflet 1	Leaflet 2	DPPC	DPPS
DPPC bilayer	0.703	84.64	84.62		
Na^+without NaCl	0.680	82.22	80.55	2.06 (1.96)	2.13
$Na^+$with 0.25N NaCl	0.640	80.91	81.65	1.95 (1.90)	1.97
Ca^{2+} without $CaCl_2$	0.677	90.24	93.94	1.60 (1.70)	1.70
Ca^{2+} with 0.25N $CaCl_2$	0.664	91.18	93.96	1.54 (1.68)	1.41

[a] Surface are per lipid corresponding to the leaflet formed only by DPPC.

[b] Mean angle between the **P**–**N** vector of DPPC head group and the outward normal to the bilayer. Error was estimated to be ∼0.05°.

[c] Hydration number around atom 10 (Fig. 1) of DPPC or DPPS. Numbers in parentheses refer to DPPC in the leaflet in the presence of DPPS.

3.3. Lipid hydration

To analyze the hydration on both leaflets of the membrane, the radial distribution function $g(r)$ (Eq. (1)) of water was calculated around the phosphate oxygen group (atom number 10 in Fig. 1). From numerical integration of the radial distribution function, the hydration numbers can be estimated for DPPC and DPPS. In order to corroborate that the system reached an equilibrated state, we studied how hydration time around the phosphate oxygen (atom 10). In this regard, we observed again how the system reached for this property a steady state after 5 ns of simulation.

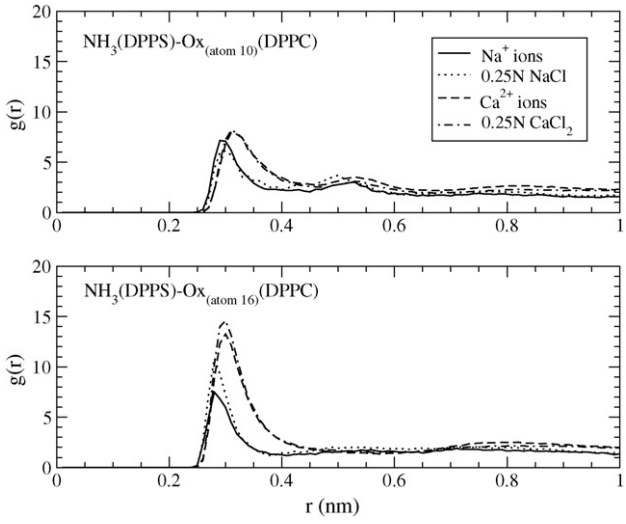

Fig. 4. Radial distribution function $g(r)$ of phosphate and carbonyl oxygens of DPPC around the ammonium NH_3group of DPPS.

Table 1 summarizes the hydration number for DPPC and DPPS for both leaflets of the membrane. From these results, we conclude that the effect of dehydration is more pronounced in the presence of calcium than sodium, for both DPPC and DPPS. In the case of DPPC, it can be seen that the degree of dehydration is almost the same, irrespective of the membrane leaflet.

3.4. Deuterium order parameter, $-S_{CD}$

The deuterium order parameter, $-S_{CD}$, obtained from ^{2}H NMR measurements reflects the order inside the membrane. This order is associated with the orientation of the hydrogen of the methylene groups at various sites on the hydrocarbon chain with respect to the normal axis to the lipid surface. Since in our simulations we did not explicitly consider the hydrogens of the methylene groups (CH_2), the order parameter ($-S_{CD}$) on the $i+1$ methylene group was defined as the unitary vector normal to the vector defined from the i to the $i+2$ CH_2 group and contained in the plane formed by the methylene groups i, $i+1$ and $i+2$. Thus, the deuterium order parameter on the ith CH_2 can be evaluated by molecular dynamics simulations using the following definition:

$$-S_{CD} = \frac{1}{2}\langle 3\cos^2(\theta) - 1\rangle \quad (2)$$

where θ is the angle between the unitary vector perpendicular to the vector from the i to the $i+2$ CH_2 group and contained in the plane formed by the i, $i+1$ and $i+2$ CH_2 plane and the z-axis. The expression in the bracket $\langle \ldots \rangle$ denotes an average of all the lipids and times. Hence, note that the $-S_{CD}$ can adopt any value in a range from −0.5 (parallel to the lipid/water interface) to 1 (oriented along the normal to the membrane surface).

Fig. 5A and B depict the order parameters of DPPC. Comparison of the experimental [48] and simulation data for the leaflet in the absence of DPPS showed good agreement. When the salt concentration increased, the order parameters increased, too, which was more noticeable in the presence of calcium. This behavior agrees with previous experimental [6] and simulation data [15] of DPPC bilayers in the presence of NaCl. This enhancement in the order parameter of the hydrocarbon tails with ionic strength is consistent with the shrinking of the surface area per lipid, as shown in Table 1. Hence, an increase in the packaging of lipids leads to an increase in the order of the lipid tails too.

As regards the order parameters of DPPS, Fig. 5C compares simulation and experimental data [49] for different salt concentrations. As can be seen, reasonable agreement was only found in pure water with sodium as counterion. For DPPS, the order parameters follow a similar trend to those obtained for the $POPS^-$ [17] in the presence of monovalent ions, where the order parameter increased with the NaCl salt concentration. However, when we looked at the effect of divalent ions on the order parameter of DPPS, the order parameter was seen to decrease in the presence of $CaCl_2$, compared with NaCl to the same normal salt concentration. This difference in behavior can be associated with the different interactions between neighboring lipids in the presence of calcium or sodium, such as it is observed from the radial distribution function between carbonyl oxygens of DPPC and NH_3 of DPPS in Fig. 4.

3.5. Lipid head group orientation

To gain insight into the effect of the presence of salt on the lipid conformation, the lipid head group orientation was measured in both lipid leaflets. Thus, the angle θ formed by the unitary **P –N** vector of a lipid head group and the z-axis perpendicular to the lipid leaflet was measured. Fig. 6 depicts the angular distribution function $f(\theta)$ for the DPPC in both leaflets of the membrane as a function of the salt concentration in solution. Leaflet 1 corresponds to the

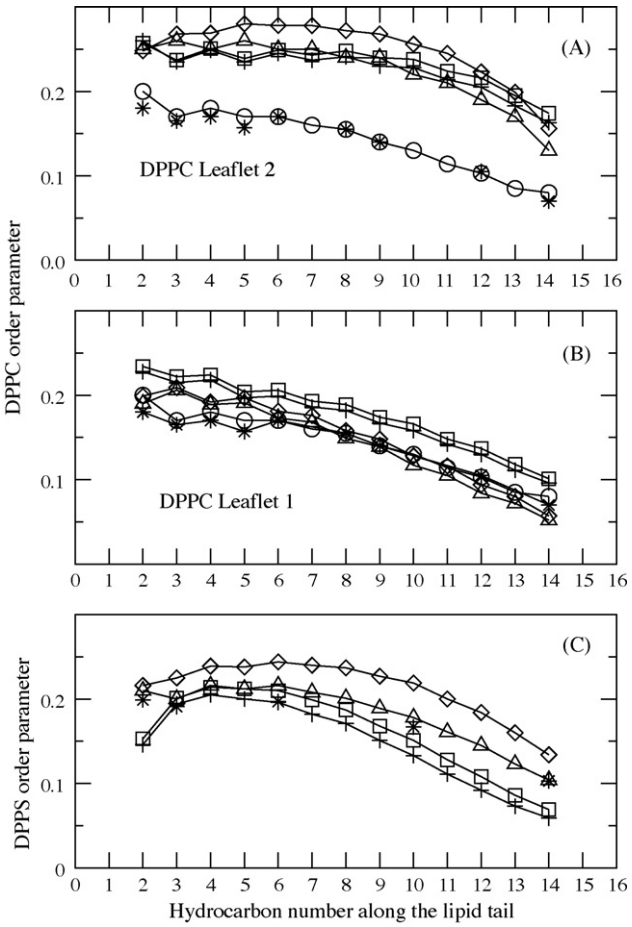

Fig. 5. Deuterium order parameters ($-S_{CD}$) calculated as average of both lipid tails. (A) DPPC leaflet 1 (B) DPPC leaflet 2 and (C) DPPS. (△) in pure water using Na^+ as counterions, (◊) 0.25N NaCl, (+) in pure water using Ca^{2+} as counterion, (□) 0.25N $CaCl_2$. The DPPC order parameters (○) of a DPPC bilayer in pure water was included as control. Experimental data (∗) of DPPC and DPPS correspond to Refs. [48] and [49], respectively.

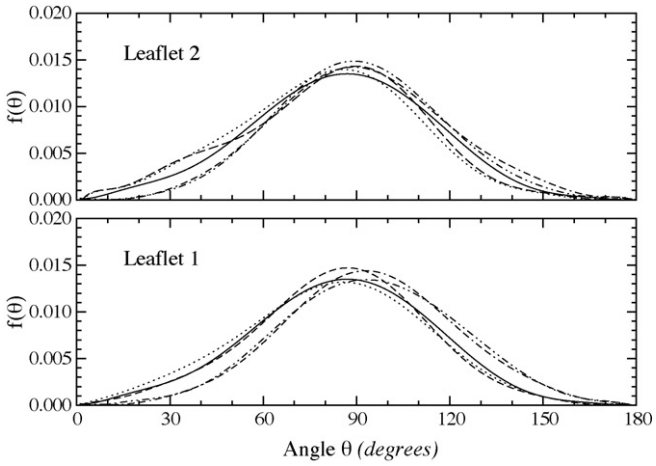

Fig. 6. Angular distribution function $f(\theta)$ of the angle formed between the **P–N** vector of DPPC and the outward normal to the bilayer, on both asymmetric membrane leaflets. Leaflet 1 corresponds to the lipid layer formed only of DPPCs and leaflet 2 to the lipid layer composed of DPPCs + DPPSs. (···) DPPC in pure water with Na^+ as counterions, (- - -) DPPC in 0.25N NaCl, (—) DPPC bilayer of control in pure water, (– ··–) DPPC in pure water with Ca^{2+} as counterions, (– – · – – –) DPPC in 0.25N $CaCl_2$.

leaflet composed of pure DPPC, while that leaflet 2 corresponds to that composed of DPPC + DPPS (see Fig. 2). From simulation data, we conclude that in both leaflets, the lipid head group orientation follows the same trend as reported by Pandit et al. [15] for a DPPC bilayer, where the **P** –**N** angle remains almost parallel to the surface of the membrane, $\theta \approx 90^{\circ}$, regardless of the salt concentration. As for the angular distribution function, Fig. 6 shows how the presence of calcium slightly modified its shape compared with that obtained in the presence of sodium, although the mean angle $\langle\theta\rangle$ was almost the same.

3.6. Translational diffusion coefficient

The two-dimensional translational diffusion coefficient $D_{t,xy}$ can be calculated from the mean-square-displacement of a certain particle as

$$\langle x^2 + y^2 \rangle = 4D_{t,xy}t \quad (3)$$

where x and y are the axes parallel to the membrane face and t the elapsed time.

Focusing our interest on estimating of the translational diffusion coefficient of ions and water from bulk solution to the phospholipid/water interface, we sliced the computational box into 19 slabs parallel to the membrane, see Fig. 2. However, due to their high mobility, both ions and water passed from one to another several times. It was not possible to estimate the precise translational diffusion coefficient of water and ions for different positions along the z-axis of the computing box and only a mean value could be estimated. This problem was circumvented by splitting the trajectory length into shorter subtrajectories of 10 ps each, and the translational diffusion coefficient calculated using Eq. (3) was assigned to the slab at the point where the center of mass (of each molecule) along the subtrajectory fall.

3.6.1. Ion translational diffusion coefficient

Fig. 7A and B shows the two-dimensional translational diffusion coefficient $D_{t,xy}$ of calcium and sodium as a function of their position along the z-axis, such as defined in Fig. 2. A diminution in the translational diffusion coefficient of $Na^+$and Ca^{2+}in the vicinity of the water–phospholipids interface can be observed. The translational diffusion coefficient of sodium falls from 4.34×10^{-5} cm^2 s^{-1} in bulk water, a value in good agreement with the experimental data of 1.34×10^{-5} cm^2 s^{-1} at 298 K [50] considering the difference in temperature, to around 0.40×10^{-5} cm^2 s^{-1} in 0.25N NaCl at both interfaces of the membrane.

For calcium, a $D_{t,xy}$ of 1.73×10^{-5} cm^2 s^{-1} was measured in bulk water, again in good agreement with the experimental data of 1.58×10^{-5} cm^2 s^{-1} reported for calcium at 298 K [50]. Finally, a $D_{t,xy}$ of 1.04×10^{-5} and 0.40×10^{-5} cm^2 s^{-1} were measured for calcium at both membrane interfaces, corresponding to the leaflet without and with DPPS, respectively, in 0.25N $CaCl_2$.

From the results mentioned above, we conclude that the presence of asymmetrically distributed DPPS leads to a noticeable asymmetry in the translational diffusion coefficient of calcium at the lipid/water interface, but almost no variation in the case of sodium ions.

3.6.2. Water translational diffusion coefficient

Fig. 7C depicts the two-dimensional translational diffusion coefficient $D_{t,xy}$ of water from bulk to the lipid/water interface, such as defined in Fig. 2. Thus in bulk water, a value of 6.2×10^{-5} cm^2 s^{-1}was measured, which is in good agreement with the value of 7.9×10^{-5} cm^2 s^{-1}measured for single point charge (SPC) water model [51] at 349 K [52]. Thus a $D_{t,xy}$ of 0.88 and 0.97×10^{-5} cm^2 s^{-1}were measured at the lipid/water interface corresponding to the absence and presence of DPPS, respectively, in 0.25N NaCl.

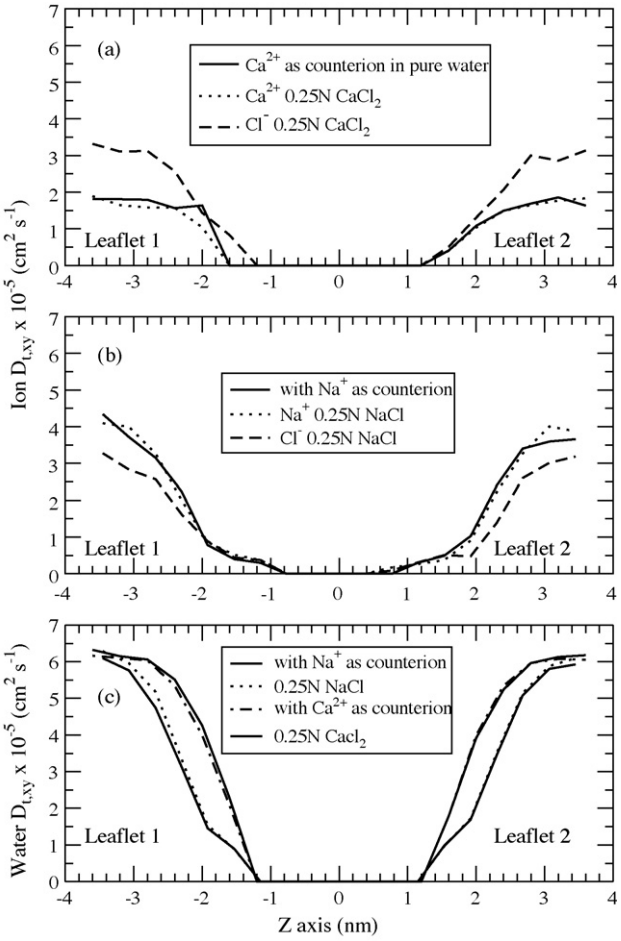

Fig. 7. Translational diffusion coefficient $D_{t,xy}$ profile of ions and water at different distance from the center of lipid bilayer (zero of the z-axis was placed in the middle of the lipid bilayer, such as defined in Fig. 2). (A) Calcium, (B) sodium and (C) water.

On the other hand a $D_{t,xy}$ of 2.27 and 1.21×10^{-5} cm^2 s^{-1} were measured for both lipid/water interfaces, corresponding to the interfaces in the absence and presence of DPPS, respectively, in 0.25N $CaCl_2$.

These results confirm that the so called *biological water layer* close to the lipid/water interface shows different behavior depending on the type of ion involved in solution and the lipid composition of the membrane.

3.7. Water relaxation time

To gain more precise insight into the dynamic behavior of water molecules as they relax from bulk to the vicinity of the lipid interface (see Fig. 2), the reorientational relaxation time of the water dipole was studied. Dynamic properties can be abstracted from other correlation functions such as the reorientational relaxation time of the water dipole, which can then be related to dielectric measurements and NMR relaxation times. This relaxation process is an example of how water in an arbitrary initial state approaches equilibrium. The characteristics of this decay are governed by interactions between molecules and by the type of motion of the particles in the system. From simulation, the reorientational relaxation time of the water dipole can be described by the correlation function $\langle P_1 \rangle$, which is defined as $\langle P_1(t) \rangle = \langle \cos \xi(t) \rangle = \langle \vec{\mu}(0) \cdot \vec{\mu}(t) \rangle$, where $\vec{\mu}$ is the unitary dipole vector of a water

molecule, and $\xi(t)$ is the angle subtended by two orientations of $\vec{\mu}$ formed as time t elapses. Furthermore, the $\langle P_1(t)\rangle$ fits a multiexponential, as follows:

$$\langle P_1(t)\rangle = \sum_{i=1}^{3} a_i e^{-(t/\tau_i)} \quad (4)$$

where τ_i corresponds to each of the correlation times and a_i is a constant of the fit associated with time τ_i. Note that even when a_i and τ_i change from fit to fit, a reproducible mean relaxation time τ_{app} can be obtained as follows:

$$\tau_{app} = \frac{\sum_{i=1}^{3} a_i \tau_i}{\sum_{i=1}^{3} a_i} \quad (5)$$

where a_i and τ_i are the values obtained from each fit.

Fig. 8 depicts the apparent rotational diffusion time of water as a function of the z-coordinate in the presence of calcium or sodium ions. In general, we observe how water slows down at the lipid/water interface compared with its behavior in bulk as a consequence of the interactions between water and phospholipid head groups. Thus, τ_{app} passes from 2.2 ps in bulk water, which is in good agreement with the experimental data of $\tau = 2.8$ ps from low frequency depolarized Raman spectroscopy (LF-RS) measurements at 340 K [53] in pure water or $\tau = 3.0$ ps measured for a SPCE water model [46] at 350 K from simulation [54], to a range of values from 10 to 23 ps depending of the side and ion present in solution. From the values of Fig. 8, the same values of τ_{app} are obtained for the leaflet in the presence of DPPS (17 and 19 ps for 0.25N $CaCl_2$ and NaCl, respectively), as for the leaflet formed only by DPPC (10 and 23 ps). From these results, we conclude that the presence of DPPS makes the dipole relaxation time independent of the type of ion in solution compared with the leaflet formed only by DPPC, in which a difference of 13 ps was measured, depending on the type of ion in solution.

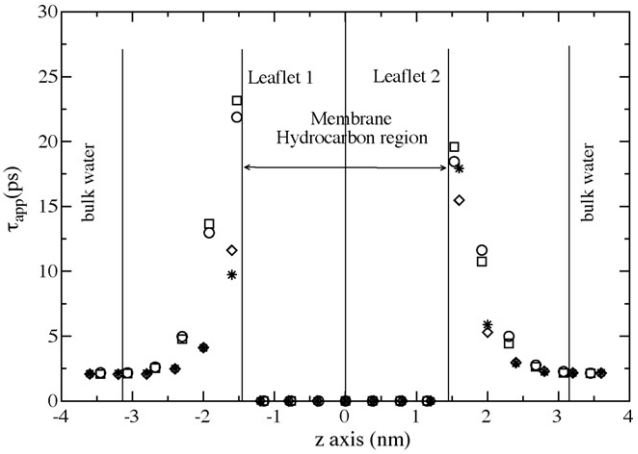

Fig. 8. Water dipole reorientational relaxation time, τ_{app}, as function of the *z-coordinate* (zero of the *z-axis* was placed in the middle of the lipid bilayer, such as defined in Fig. 2). (○) with Na^+ as counterions in pure water, (□) in 0.25N NaCl, (◊) with Ca^{2+} as counterions in pure water and (∗) in 0.25N $CaCl_2$.

3.8. Ion-lipid residence time

Fig. 9 depicts the radial distribution function ($g(r)$) of sodium and calcium around the phosphate oxygen of DPPC for both leaflets of the membrane (atom 10, Fig. 1). Based on the height of the peaks of these coordination functions in Fig. 9, Ca^{2+} is clearly much more coordinated to phosphate oxygen than Na^+, as observed from Fig. 2, where most of calcium ions penetrated into the region B, corresponding to the lipid heads, preferentially in the leaflet in presence of DPPS.

To gain insight into the ion coordination to lipids, we studied the mean residence time of sodium and calcium ions around the phos-

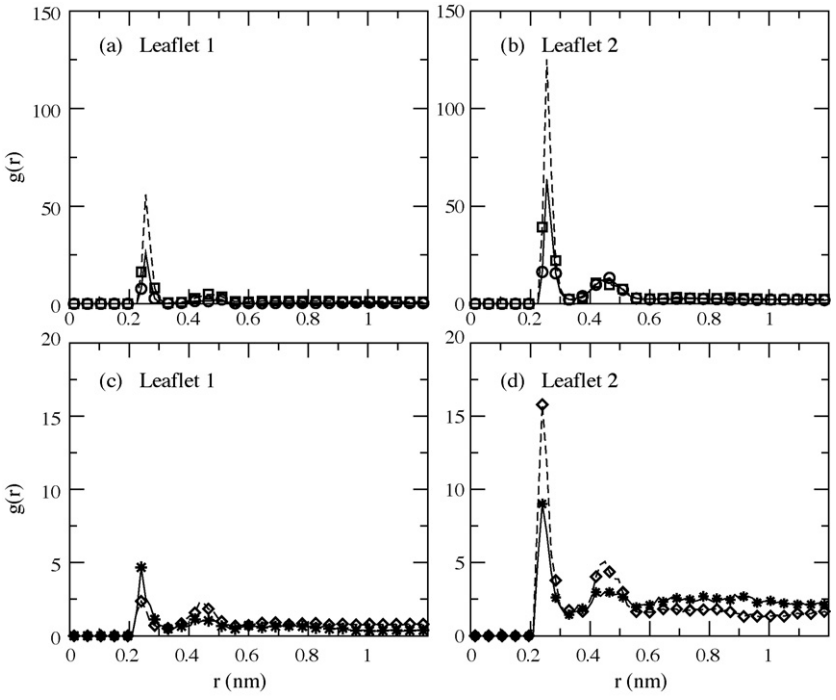

Fig. 9. Radial distribution function of calcium (A and B) and sodium (C and D) around DPPC phosphate oxygen in both membrane leaflets.(○) in water with Ca^{2+} as counterions, (□) in 0.25N $CaCl_2$, (∗) in water with Na^+ as counterions and (◊) in 0.25N $CaCl_2$.

Table 2
Residence time (in ps) of sodium and calcium ions around the phosphate and carbonyl oxygens of DPPC on both membrane leaflets, in the absence and presence of DPPS, respectively.

	Mean residence time (ps)	
	Leaflet 1 (DPPC)	Leaflet 2 (DPPC + DPPS)
Phosphate oxygen (atom 10, Fig. 1)		
Na^+ without salt	1.34	4.56
Na^+ + 0.25N NaCl	1.85	6.04
Ca^{2+} without salt	0.91	19.32
Ca^{2+} + 0.25N $CaCl_2$	1.30	16.60
Carbonyl oxygen (atom 16, Fig. 1)		
Na^+ without salt	1.23	4.67
Na^+ + 0.25N NaCl	1.93	4.25
Ca^{2+} without salt	0.82	15.78
Ca^{2+} + 0.25N $CaCl_2$	1.05	15.95

phate and carbonyl oxygens of DPPC (atoms 10 and 16 of Fig. 1), defined as the average time that a given ion spends in the coordination shell. Table 2 shows the mean residence time of sodium and calcium around phosphate oxygen (atom 10, Fig. 1) and carbonyl oxygen (atom 16, Fig. 1). From these data, it can be appreciated how the residence time of sodium and calcium remained almost constant for the leaflet in the absence of DPPS. However, in the leaflet formed by DPPC and DPPS, the residence time noticeably increased compared with the leaflet formed only by DPPC. Thus, the residence time of calcium at the DPPC/DPPS interface becomes more than one order of magnitude greater than in the leaflet formed only by DPPC.

4. Conclusions

The molecular dynamics simulations technique was employed to study the structure and dynamics of an asymmetric phospholipid bilayer in its liquid crystalline state, in the presence of monovalent or divalent ions. The asymmetric bilayer was generated by two leaflets, where one was composed of pure DPPC and the another of a mixture of DPPC and DPPS. From the analysis of the simulated trajectories, we observed how the asymmetry of the membrane affects the lipid properties and how these properties are affected by the type and concentration of ion present in solution. Thus, the presence of Na^+ or Ca^{2+} in solution produce a shrinking of the lipid surface. Our results indicated that calcium ions interacted more strongly with both phospholipids, DPPC and DPPS, than sodium ions. Thus, this shrinking of the lipid surface (i.e. an increase in lipid packaging) is reflected by an increase in the order parameters of the lipid tails, $-S_{CD}$ of DPPC. On the other hand, the presence of calcium reduces the order parameter of DPPS, which follows a different trend from DPPC in the case of both membrane leaflets. In this respect, it was observed how the increase in the order of DPPC is enhanced by the presence of DPPS, independently of the type of ion present in solution.

The lipid head group orientation is slightly affected by the type of ion present in solution. The presence of DPPS modifies the shape of the angular lipid head group distribution function, to an extent that depends on the type and concentration of the ion present in solution.

Further to the results discussed above, properties such as lipid–lipid and lipid-hydration of DPPC were also strongly affected by the presence of DPPS. These differences between the DPPC of opposite leaflets were enhanced by the ionic strength of the solution. In summary, an increase in the salt concentration in solution asymmetrically perturb the properties of DPPC on both leaflets. Thus, we conclude that the behavior measured for DPPC in one leaflet can not be directly correlated with the lipid behavior on the opposite leaflet.

Regarding the lipid/water interface, we conclude that the translational diffusion coefficient ($D_{t,xy}$) and the reorientational relaxation time (τ_{app}) at the interface diminish with respect to the bulk water. In addition, it was seen how the asymmetry of the membrane introduces a noticeable diminution in the translational and the reorientational relaxation time of water in the interface of the leaflet composed by DPPC + DPPS compared with the opposite one formed only by DPPC. Such behavior was more strongly affected by the presence of calcium than of sodium.

Thus, from all the results shown above, we conclude that the presence of 30% DPPS in one of the two leaflets (similar to the ratio of charged lipids in a cellular membrane) introduces substantial changes in the membrane properties, which in turn, are strongly dependent on the type and concentration of the ions present in solution.

Acknowledgments

Authors wish to thank Fundacion Seneca de la Region de Murcia the financial support through the project 08647/PPC/08. RDP is a member of 'Carrera del Investigador', CONICET, Argentina. We also wish to acknowledge the assistance of the Computing Center of the Polytechnic University of Cartagena (SAIT).

References

[1] P. Yeagle (Ed.), The Structure of Biological Membranes, CRC Press, Inc., 1991.
[2] J. Weitzman, J. Biol. 3 (2004) 1.
[3] V. Fadok, D. Bratton, D. Rose, A. Pearson, R. Ezekewitz, P. Henson, Nature (2000) 85.
[4] N. Kato, M. Nakanishi, N. Hirashima, Biochemistry 41 (2002) 8068.
[5] C. Altenbach, J. Seelig, Biochemistry 23 (1984) 3913.
[6] H. Binder, O. Zschoring, Chem. Phys. Lipids 115 (2002) 39.
[7] W.F. van Gunsteren, H.J.C. Berendsen, Angew. Chem. Int. Ed. Engl. 29 (1990) 992.
[8] D. Frenkel, B. Smit, Understanding Molecular Simulations, Academic Press, 2002.
[9] D. Bassolino-Klimas, H. Alper, T. Stouch, Biochemistry 32 (1993) 12624.
[10] H. Heller, M. Schaefer, K. Schulten, J. Phys. Chem. 97 (1993) 8343.
[11] H.E. Alper, D. Bassolino-Klimas, T.R. Stouch, J. Chem. Phys. 99 (1993) 5554.
[12] E. Egberts, S.J. Marrink, H.J.C. Berendsen, Eur. Biophys. J. 22 (1994) 423.
[13] D. Tieleman, S. Marrink, H. Berendsen, Biochim. Biophys. Acta (BBA) 1331 (1997) 235.
[14] J.J. López Cascales, J. García de la Torre, S. Marrink, H. Berendsen, J. Chem. Phys. 104 (1996) 2713.
[15] S. Pandit, D. Bostick, M. Berkowitz, Biophys. J. 84 (2003) 3743.
[16] R.A. Bockmann, H. Grubmuller, Angew. Chem. 43 (2004) 1021.
[17] P. Mukhopadhyay, L. Monticelli, D. Tieleman, Biophys. J. 86 (2004) 1601.
[18] J. Sachs, H. Nanda, H. Petrache, T. Woolf, Biophys. J. 86 (2004) 3772.
[19] K. Shinoda, W. Shinoda, M. Mikami, Phys. Chem. Chem. Phys. 9 (2007) 643.
[20] A. Gurtuvenko, I. Vattulainen, J. Phys. Chem. B 112 (2008) 1953.
[21] U. Pedersen, C. Laidy, P. Westh, G. Peters, Biochim. Biophys. Acta 1758 (2006) 573.
[22] J. Faraudo, A. Travesset, Biophys. J. 92 (2007) 2806.
[23] Y. Inoko, T. Yamaguchi, K. Furuya, T. Mitsui, Biochim. Biophys. Acta 413 (1975) 24.
[24] L. Lis, V. Parsegian, R. Rand, Biochemistry 20 (1981) 1761.
[25] L. Lis, W. Lis, V. Parsegian, R. Rand, Biochemistry 20 (1981) 1771.
[26] L. Herbette, C. Napolitano, R. McDaniel, Biophys. J. 46 (1984) 677.
[27] S. Tatulian, V. Gordeliy, A. Sokolova, A. Syrykh, Biochim. Biophys. Acta 1070 (1991) 143.
[28] N. Yamada, H. Seto1, T. Takeda, M. Nagao, Y. Kawabata, K. Inoue, J. Phys. Soc. Jpn. 74 (2005) 2853.
[29] M. Ganesan, D. Schwinke, N. Weiner, Biochim. Biophys. Acta 686 (1982) 245.
[30] R. Lehrmann, J. Seelig, Biochim. Biophys. Acta 1189 (1994) 89.
[31] H. Akutsu, J. Seelig, Biochemistry 20 (1981) 7366.
[32] T. Shibata, Chem. Phys. Lipids 53 (1990) 47.
[33] D. Huster, K. Arnold, K. Gawrisch, Biophys. J. 78 (2000) 3011.
[34] J. Marra, J. Israelachvili, Biochemistry 24 (1985) 4608.
[35] S. Tatulian, Eur. J. Biochem. 170 (1987) 413.
[36] K. Satoh, Biochim. Biophys. Acta 1239 (1995) 239.
[37] J.J. López Cascales, T.F. Otero, B.D. Smith, C. Gonzalez, M. Marquez, J. Phys. Chem. B 110 (2006) 2358.
[38] H. Berendsen, D. van der Spoel, R. van Drunen, Comp. Phys. Commun. 91 (1995) 43–56.
[39] E. Lindahl, B. Hess, D. van der Spoel, J. Mol. Model. 7 (2001) 306.
[40] T. Darden, D. York, L. Pedersen, J. Chem. Phys. 98 (1993) 10089.
[41] U. Essmann, L. Perea, M. berkowitz, T. Darden, H. Lee, L. Pedersen, J. Chem. Phys. 103 (1995) 8577.

[42] A. Seelig, J. Seelig, Biochemistry 13 (1974) 4839.
[43] L.R. De Young, K.A. Dill, Biochemistry 27 (1993) 5281.
[44] G. Cevc, A. Watts, D. Marsh, Biochemistry 20 (1981) 4955.
[45] H. Hauser, F. Paltauf, G.G. Shipley, Biochemistry 21 (1982) 1061.
[46] H. Berendsen, J. Grigera, T. Straatsma, J. Phys. Chem. 91 (1987) 6269.
[47] J. Nagle, S. Tristam-Nagle, Biochim. Biophys. Acta 1469 (2000) 159.
[48] M.F. Brown, J. Phys. Chem. 77 (1982) 1576.
[49] J.L. Browning, J. Seelig, Biochemistry 19 (1980) 1262.
[50] D. Lide (Ed.), Handbook of Chemistry and Physics, CRC, 2002–2003.
[51] H.J.C. Berendsen, J.P.M. Postma, W.F. van Gunsteren, J. Hermans, in: B. Pullman (Ed.), Intermolecular Forces, Reidel, Dordrecht, 1981, p. 331.
[52] J. Postma, A molecular dynamics study of water, Ph.D. Thesis, Rijkuniversiteit Groningen, The Netherlands (1985).
[53] K. Mizoguchi, T. Ujike, Y. Tominaga, J. Chem. Phys. 109 (1998) 1867.
[54] S. Balasubramanian, B. Bagchi, J. Phys. Chem. B 106 (2002), 3668.